DOI: 10.5604/01.3001.0053.4035
Volume 116 • Issue 2 • February 2023
Journal of Achievements in Materials and Manufacturing Engineering
International Scientific Journal published monthly by the World Academy of Materials and Manufacturing Engineering

Study of selected properties of PLA used in 3D printing

K. Sośniak [a], D. Biela [a,*], D. Szalaty [a], M. Ścieszka [a], M. Polok-Rubiniec [b], A. Włodarczyk-Fligier [b], A. Kania [b]

[a] Students of the Faculty of Mechanical Engineering, Silesian University of Technology, Akademicka 2A, 44-100 Gliwice, Poland

[b] Department of Engineering Materials and Biomaterials, Faculty of Mechanical Engineering, Silesian University of Technology, Konarskiego 18a, 44-100 Gliwice, Poland

* Corresponding e-mail address: dawidbiela@op.pl

ORCID identifier: https://orcid.org/0000-0001-8940-0147 (M.P.-R.)

ABSTRACT

Purpose: This study focuses on determining the best possible structure of the orthosis made with FDM 3D printing technology. To produce the samples, a thermoplastic PLA material was selected that met the conditions of biodegradability, biocompatibility and non-toxicity. The samples produced were subjected to a tensile strength test and corrosion resistance.

Design/methodology/approach: Studies based on FEM analysis were carried out using the advanced engineering software CAE - Inventor. The samples were designed in the CAD system, while the G-Code path was generated using the PrusaSlicer 2.5.0 program dedicated to the Prusa i3 MK3S+ printer, which was used to create the models. Surface morphology observations of PLA were carried out with a Zeiss SUPRA 35 scanning electron microscope (SEM). The static tensile test was performed on the Zwick/Roell z100 device based on the PN-EN ISO 527:1 standard. Electrochemical corrosion tests were carried out using the Autolab PGSTAT302N Multi BA potentiostat in Ringer solution at a temperature of 37°C.

Findings: The research allowed the appropriate structure of the orthosis made of PLA polymer material using 3D FDM printing technology. The static tensile test, SEM and corrosion tests confirmed the correct application of this material for the selected purpose. It was possible to determine that samples with holes of 10 mm had the highest strength properties. Due to the tensile tests, the average tensile strength of those samples was around 61 MPa. The corrosion parameters of PLA were determined using Tafel analysis.

Research limitations/implications: The research methodology proposed in work can be used to study other biomedical materials. The results presented can be the basis for further tests in order to search for the best orthopaedic stabiliser.

Originality/value: The innovative part of the article are three different versions of structures intended for making orthoses used in medicine.

Keywords: Materials, Biomaterials, PLA, 3D printing, FEM

Reference to this paper should be given in the following way:

K. Sośniak, D. Biela, D. Szalaty, M. Ścieszka, M. Polok-Rubiniec, A. Włodarczyk-Fligier, A. Kania, Study of selected properties of PLA used in 3D printing, Journal of Achievements in Materials and Manufacturing Engineering 116/2 (2023) 72-79. DOI: https://doi.org/10.5604/01.3001.0053.4035

BIOMEDICAL AND DENTAL ENGINEERING AND MATERIALS

1. Introduction

Polylactide (PLA) belongs to the thermoplastic polymer group and is obtained from raw materials of natural origin. It is characterised by good mechanical properties, similar to popular polymers such as PET (polyethylene terephthalate) and PS (polystyrene) (Tab. 1). PLA is biodegradable, biocompatible and non-toxic. Due to the above properties, it has been used in a wide range of industries [1].

Many years of research on PLA led to the determination of many of its properties [2]. The main factor influencing its properties is the component stereochemical composition of repeating units and distribution along the polyester chain. Multimolecular PLA is a stereoregular, isotactic polymer with a glass transition temperature of T_g = 55-65°C and a melting point of T_t = 170-183°C. Atactic PLA (PLLA/PDLA) built of heterochiral PLDLA units is an amorphous polymer with a T_g = 59°C, which does not have a melting point. On the other hand, a mixture of homochiral PLLA and PDLA chains can form stereo-complexes with a melting point <230°C [3].

However, medicine and pharmacy are the most important fields in which PLA has been used. These areas require high accuracy and should comply with many safety standards [4,5]. PLA guarantees non-toxicity in case of contact with the body. In addition, the decomposition process in the body is quite short and does not have a negative impact on any tissues or organs. After a certain time, polylactide decomposes to non-toxic [1,6,7].

In the case of orthopaedics, metal implants are aimed at the mechanical strengthening of the bone structure. It was associated with the need for a second surgery to remove the implant. When PLA is used, it is guaranteed that after the recovery period, the material will automatically dissolve in the body without causing negative effects on the bone structure. In addition, threads and stitches made of this material have been used for internal and external treatments to prevent additional procedures related to their removal [1].

When it comes to tissue reconstruction, polylactide is used to build a polymer scaffolding on which cells will be seeded. After the recovery period, the scaffolding is reabsorbed. Furthermore, the polymeric material is enriched with substances that favour the growth of tissues [8,9].

2. Methodology

2.1. Finite elements method

Studies based on FEM (Finite Elements Method) analysis were carried out using advanced engineering software from Autodesk – Inventor. First, geometric models of individual samples were created in the CAD system. In the next step, geometrical models were assigned material properties that define polylactide. Then, in the stress analysis environment of the Inventor package, the initial and boundary conditions were formulated, consisting of assigning restraints and setting specific loads. The last stage before the analysis was the imposition of a finite element mesh consisting of linear tetrahedral elements defined by four corner nodes connected by six straight edges. The created mesh was additionally compacted in places of narrowings and sharp bends, i.e. in areas most exposed to stress concentration. The prepared models were subjected to FEM analysis, and results of reduced stresses were derived according to the von Misses hypothesis and displacements. The parameters related to the grid settings are shown in Table 2 [10].

Table 2.
Grid size settings

No.	Parameter	Value
1.	Average element size	0.1
2.	Min. element size	0.2
3.	Gradation factor	1.5

Table 1.
PLA properties [1]

No.	Parameter	PLA	PLLA	PLDLA
1.	Density, g/cm^3	1.25	1.30	1.27
2.	Tensile strength, MPa	60	95	50
3.	Young's module, GPa	3.5	4.14	3.45
4.	Elongation at break, %	2.5-6	3.0-10	2.0-10
5.	Glass transition temperature T_g, °C	45-60	55-65	50-60
6.	Melting temperature T_t, °C	150-162	170-200	Amorphous (lack of T_t)

A force exerting pressure on the middle, upper part of the model with a value of 100 N was also defined, and fixed constraints were determined for the four side walls of the model. The last stage, before the FEM analysis, was to determine the detailed properties of the material that defines polylactide (PLA), the parameters of which are listed in Table 3.

Table 3.
Material properties of the PLA

No.	Parameter	Value
1.	Young's module, GPa	3.5
2.	Poisson's ratio	0.33
3.	Kirchhoff module, MPa	1202
4.	Density, g/cm^3	1.3
5.	Yield strength, MPa	45
6.	Tensile strength, MPa	60

2.2. 3D printing

The process of 3D printing started with modelling the geometry of the samples according to PN-EN ISO 527-1 standard. Next, the CAD models were exported to *.stl format in order to implement the model in PrusaSlicer 2.5.0. The software was used as a tool to divide the object into layers, prepare print parameters (Tab. 4) and generate a G-Code path (Fig. 1).

Table 4.
3D printer settings

No.	Parameter	Value
1.	Nozzle diameter, mm	0.4
2.	Nozzle temperature, °C	215
3.	Bed temperature, °C	55
4.	Layer height, mm	0.2
5.	First layer height, mm	0.2
6.	Fill density, %	100
7.	Fill pattern	Rectilinear

The samples were printed on a Prusa i3 MK3S+ printer in a closed room at a temperature of 22 °C. The device had no thermal chamber, and all samples were made from one filament spool.

2.3. Structural analysis

Observations of printing PLA surface morphology were carried out using a Zeiss SUPRA 35 scanning electron microscope (SEM). SEM images were obtained using an SE mode and an accelerating voltage of 5.0 kV.

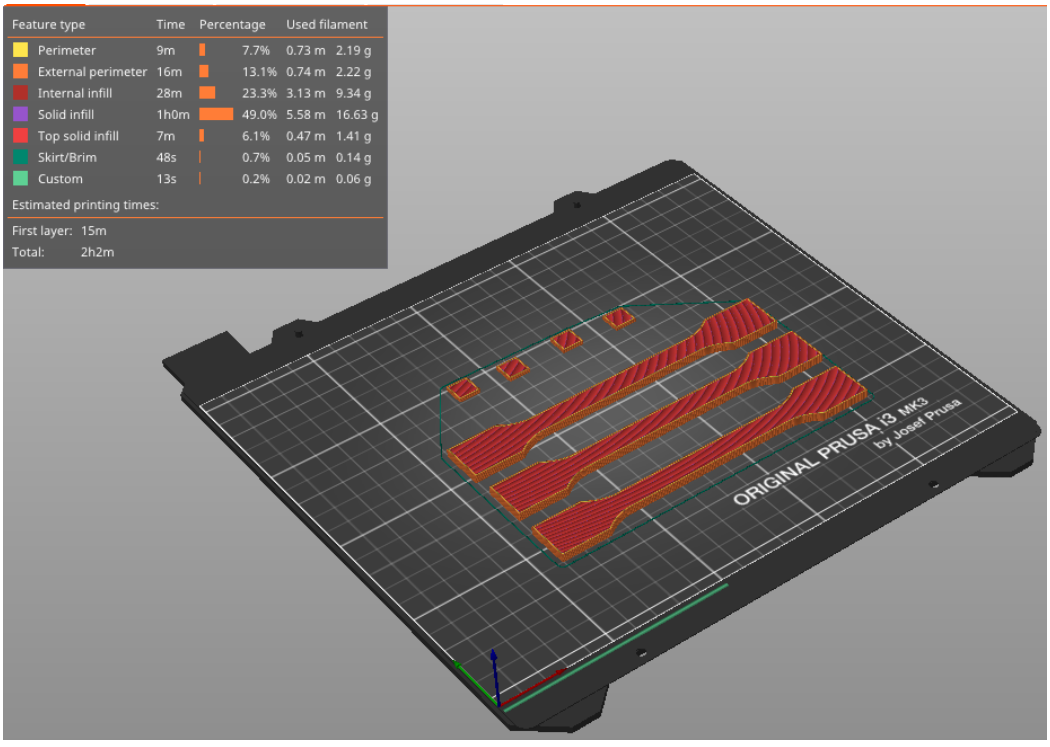

Fig. 1. Preparing 3D printing models in PrusaSlicer 2.5.0

2.4. Corrosion study

Electrochemical corrosion tests were performed using an Autolab PGSTAT302N Multi BA potentiostat. A platinum rod was used as the counter electrode, and a saturated calomel electrode was used as the reference electrode. The experiment was carried out at a temperature of 37°C in Ringer solution (8.6 $g \cdot dm^{-3}$ NaCl, 0.3 $g \cdot dm^{-3}$ KCl, 0.48 $g \cdot dm^{-3}$ $CaCl_2 \cdot 6H_2O$). In order to stabilize the samples before testing, they were immersed in the Ringer solution for 60 minutes. Tafel analysis was adopted to determine corrosion parameters, such as, for example, corrosion potential – E_{corr}, corrosion current density – j_{corr} and polarization resistance – R_p.

For the electrochemical tests, the square samples with a testing area of 1 cm^2 and a thickness of 2 mm have been prepared.

2.5. Static tensile test

The conditions and method of the static tensile test for plastics are described in the PN-EN ISO 527:1 standard, called 'Plastics – Determination of tensile properties'. The dimensions of the sample should be taken as follows: thickness 2 ± 0.2mm, width of the measuring part 10 ± 0.2 mm and a total length over 150 mm (Fig. 2 and Tab. 5).

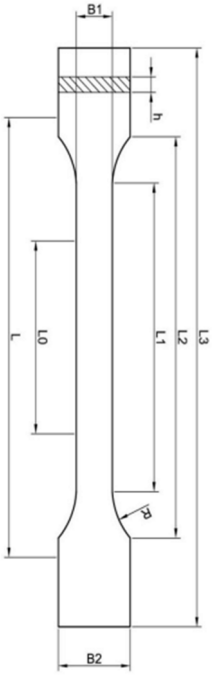

Fig. 2. Specimen dimensions according to the PN-EN ISO 527:1 standard

Table 5.
Specification of type A specimen

No.	Type A Specimen	Dimensions, mm
1.	B1 – Width of narrow section	10
2.	B2 – Width overall	20
3.	L – Distance between grips	115
4.	L0 – Gage length	50
5.	L1 – Length of narrow section	80
6.	L2 – The distance between wide parallel located parts	104
7.	L3 – Length overall	150
8.	R – Radius of fillet	22
9.	h – Thickness	2

The tests were carried out on a Zwick/Roel z100 tensile test machine. The sample was stretched at a traverse speed of 1 mm/min. The test was carried out until the sample was destroyed. The deformation and stress values were also derived from the static tensile test. In addition, graphs were generated to illustrate the values [11].

3. Results and discussion

The Von Misses stresses, displacements, and safety factors were determined in the FEM analysis. The highest stresses for each of the models were observed to occur close to their outer edges, in the vicinity of the restraint points. A high-stress value can also be seen where the force is applied. The largest displacements are visible in the middle part of the models. Their value decreases significantly inversely proportional to the distance from the application of the force. The analysis also allowed determining the safety factor. The graphical results of all the analyses carried out are presented in Figures 3-5, and the numerical values are summarised in Table 6. The strength parameters of the previously prepared models were verified in the static tensile test. The test results are summarized in Table 6.

Table 6.
Parameter values obtained by FEM analysis

No	Model number	1	2	3
1.	Max principal stress, MPa	29.09	19.58	26.02
2.	Max displacement, mm	1.26	0.95	1.08
3.	Min. safety factor	1.2	2.11	1.55

a) b)

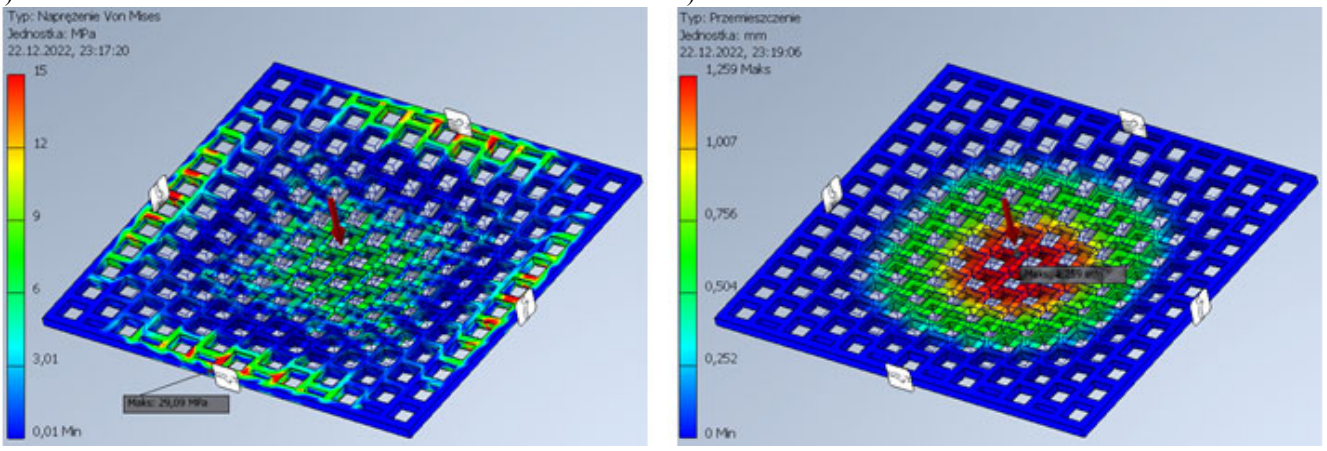

Fig. 3. Graphical stress (a) and displacements (b) results for model number 1

a) b)

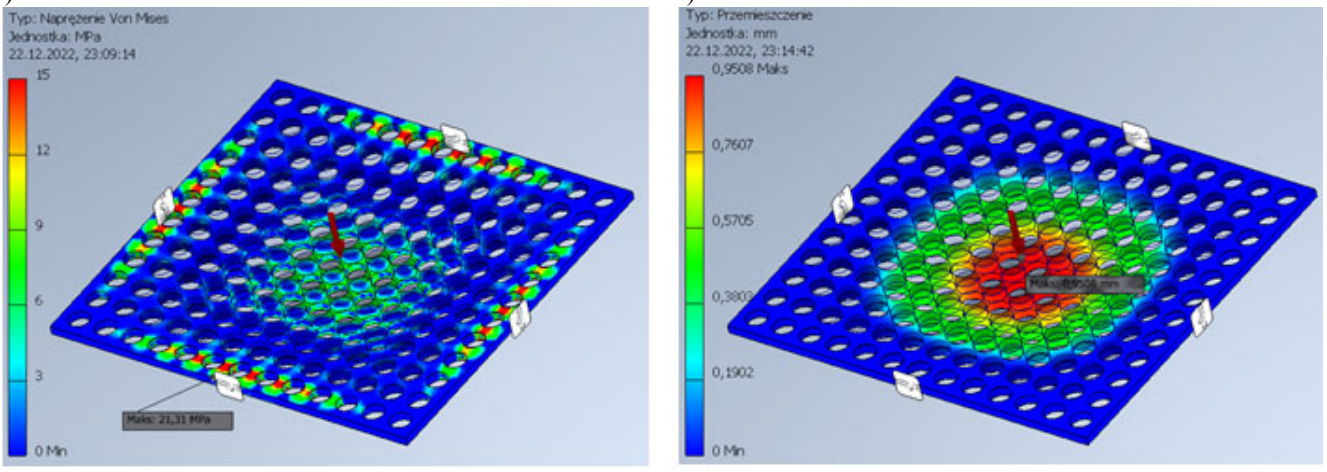

Fig. 4. Graphical stress (a) and displacements (b) results for model number 2

a) b)

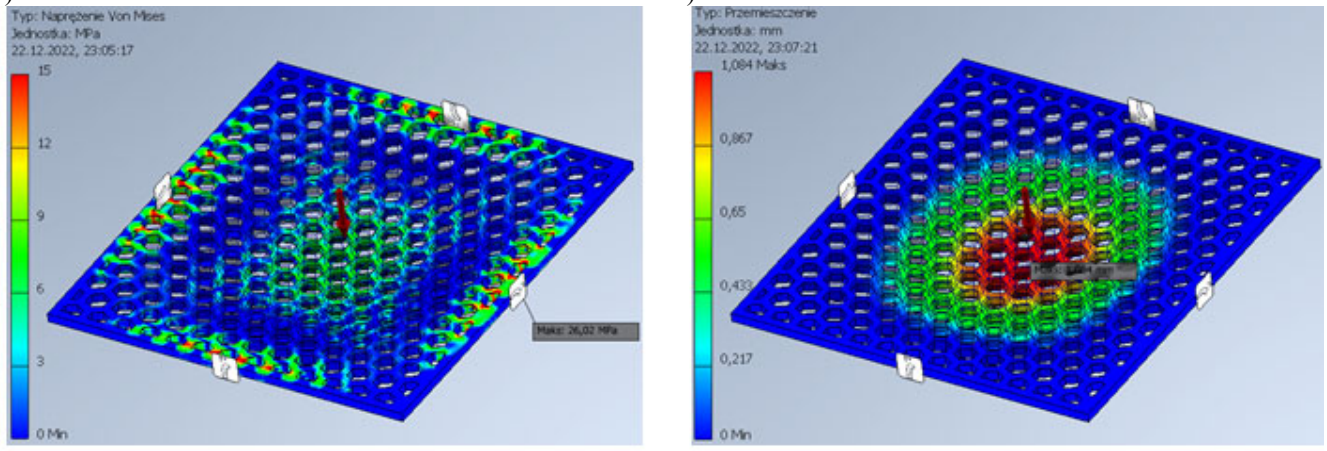

Fig. 5. Graphical stress (a) and displacements (b) results for model number 3

The analysis shows that the second model, whose structure is made up of 10 mm diameter holes, is characterized by the lowest values of Von Misses stresses and displacements, as well as the highest safety factor. This suggests that the second structure is optimal. Taking into account the concentrated force of 100 N, model 1 with a structure in the form of squares has the worst parameters.

Figure 6 shows the morphology of the PLA surface with different magnifications. On the basis of the observation results, it was found that the PLA structure is heterogeneous with slight surface deformations.

a)

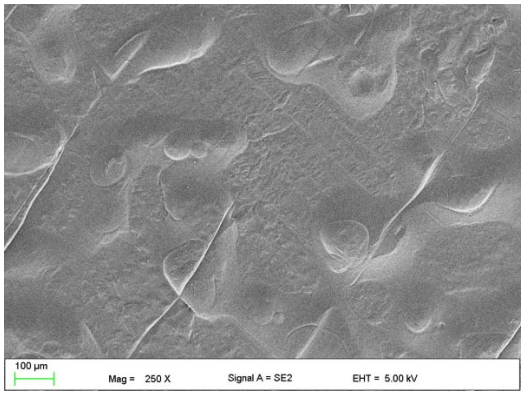

b)

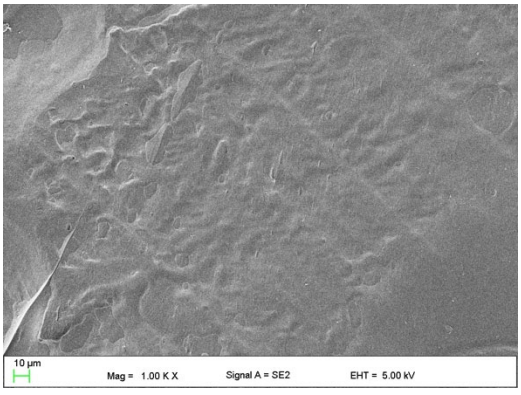

Fig. 6. Surface morphology of PLA

The strength parameters of the prepared models were verified in the static tensile test. The test results are summarized in Table 7 and are presented graphically in Figure 7.

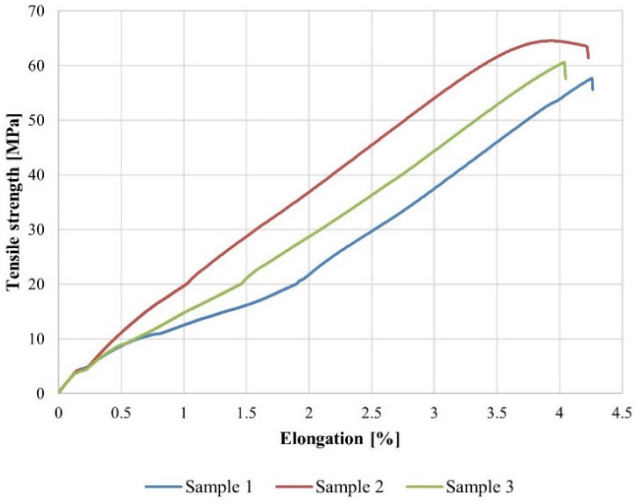

Fig. 7. Static tensile test results

The static tensile test showed properties as expected. Similar values can be found in other studies [12,13]. Müller et al. studied the PLA material with natural bamboo filler printed by 3D printing technology. The authors also stated that infill density has a significant effect on the tensile strength of the samples.

The tensile strength value of three samples with the same density is similar, and the average strain is 61 MPa. The samples break at an average elongation of 4.1%. It can be seen from the graph that the material does not have a clear yield point.

Slightly lower tensile strength values for PLA and PLA with Coconut wood (with a 75% infill percentage) were obtained by Kananathan et al. [13]. The R_m for the PLA was 37.55 MPa, while for PLA/Coconut wood was 19.35 MPa.

Table 7.
Results of static tensile tests

No.	σ_M, MPa	ε_M, %	ε_{tM}, %	σ_B, MPa	ε_B, %	ε_{tB}, %	b, mm	h, mm	A_0, mm^2
1.	57.7	4.3	4.3	57.7	4.3	4.3	10	2	20
2.	64.5	3.9	3.9	64.5	3.9	3.9	10	2	20
3.	60.6	4.0	4.0	60.6	4.0	4.0	10	2	20
Average values									
-	61.0	4.1	4.1	61.0	4.1	4.1	10	2	20

The corrosion resistance of PLA was studied using electrochemical tests. The potentiodynamic curve in corrosion tests gives information about the corrosion behaviour of studied PLA. Corrosion tests were performed in Ringer solution, in an environment that simulates the human body, at a temperature of 37°C. The polarization curve of the PLA is shown in Figure 8.

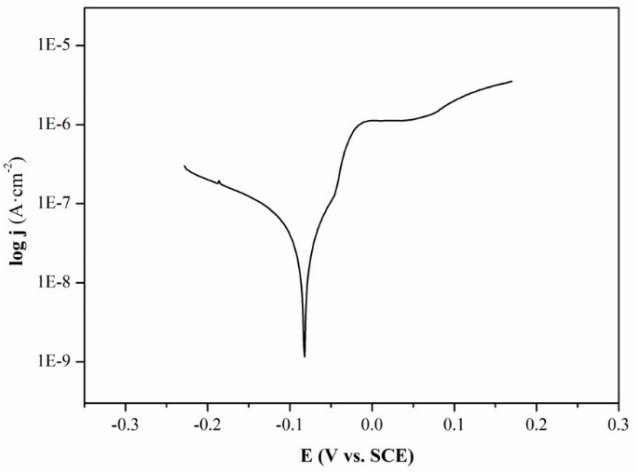

Fig. 8. Polarization curve for the PLA in Ringer solution at 37°C

Based on the results presented, it can be stated that the cathode curve, located on the left side of the graph, was in a higher current range compared to the anode curve. This may suggest a good corrosion resistance of the PLA material. Tafel extrapolation of the polarization curve determined the basic corrosion parameters of PLA: corrosion potential (E_{corr}), which is -79 mV, polarization resistance (R_p) equals 386 kΩ·cm^2, and corrosion current density (j_{corr}) 0.1 mA·cm^{-2}. Similar results obtained Carbajal-De la Torre et al. [14]. They studied the corrosion activity of scaffolds composed of bioactive glass and PLA. The tests were carried out in Hank's and SBF (Simulated Body Fluid) saline solutions. The values of corrosion current densities were between 0.1 to 0.3 μA·cm^{-2}, and they were lower than j_{corr} of 316L SS matrix (j_{corr} was 733 μA·cm^{-2}) under similar conditions.

4. Conclusions

Based on the results presented, it can be concluded that biodegradable polymer such as PLA is promising biomaterial used for orthosis.

On the basis of the surface morphology of PLA observations carried out in SEM, it was shown that the PLA structure was heterogeneous.

As a result of the three models made in the CAD program using FEM analysis, it was stated that the best strength properties characterized the sample with holes with a diameter of 10 mm.

The results of the tensile strength tests showed that the average R_m was 61 MPa, while the elongation was 4.1%.

The results of potentiodynamic tests also suggest that the biopolymer has good anti-corrosion properties.

The research results obtained in the work will be the basis for further investigations in the search for the best orthopaedic stabilizer.

Additional information

This article was funded by the Project Based Learning (PBL) realized at the Silesian University of Technology.

References

[1] P. Ruśkowski, Polylactide in medical applications, Plastics in Industry 2 (2017) 22-28 (in Polish).
[2] A. El Magri, Optimizing the mechanical properties of 3D-printed PLA-graphene composite using response surface methodology, Archives of Materials Science and Engineering 112/1 (2021) 13-22. DOI: https://doi.org/10.5604/01.3001.0015.5928
[3] B. Nowak, Polylactide (PLA) biodegradation, Archives of Waste Management and Environmental Protection 2 (2010) 1-10 (in Polish).
[4] A.D. Dobrzańska-Danikiewicz, T.G. Gaweł, M. Karska, Manufacturing of metal-polymer composites for medical applications, Archives of Materials Science and Engineering 89/1 (2018) 9-19. DOI: https://doi.org/10.5604/01.3001.0011.5725
[5] D.J. dos Santos, L.B. Tavares, J.R. Gouveia, G.H. Batalha, Lignin-based polyurethane and epoxy adhesives: a short review, Archives of Materials Science and Engineering 107/2 (2021) 56-63. DOI: https://doi.org/10.5604/01.3001.0015.0242
[6] W. Szlezynger, Z.K. Brzozowski, Plastics. Special and engineering polymers, vol. 2, Fosze, Rzeszow, 2012 (in Polish).
[7] M.A. Woodruff, D.W. Hutmacher, The Return of a Forgotten Polymer – Polycaprolactone in the 21st Century, Progress in Polymer Science 35/10 (2010) 1217-1256. DOI: https://doi.org/10.1016/j.progpolymsci.2010.04.002
[8] A. Kruk, A. Gadomska-Gajadhur, P. Ruśkowski, A. Chwojnowski, L. Synoradzki, Preparation of polylactide cell scaffolds with a spongy structure –

preliminary research and process optimization, Polymers 62/2 (2017) 118-126 (in Polish). DOI: https://doi.org/10.14314/polimery.2017.118

[9] V.C. Pinto, T. Ramos, S. Alves, J. Xavier, P. Tavares, P.M.G.P. Moreira, R.M. Guedes, Comparative Failure Analysis of PLA, PLA/GNP and PLA/CNT-COOH Biodegradable Nanocomposites thin Films, Procedia Engineering 114 (2015) 635-642. DOI: https://doi.org/10.1016/j.proeng.2015.08.004

[10] G. Krzesiński, T. Zagrajek, P. Marek, P. Borkowski, The finite element method in the mechanics of materials and structures, Publishing House of the Warsaw University of Technology, Warsaw, 2015 (in Polish).

[11] B. Goichi, K. Yuichi, N. Keita, A. Yoshio, Examination of heat resistant tensile properties and molding conditions of green composites composed of kenaf fibers and PLA resin, Advanced Composite Materials 16/4 (2007) 361-376. DOI: https://doi.org/10.1163/156855107782325203

[12] M. Müller, P. Jirku, V. Šleger, R.K. Mishra, M. Hromasová, J. Novotný, Effect of Infill Density in FDM 3D Printing on Low-Cycle Stress of Bamboo-Filled PLA-Based Material, Polymers 14/22 (2022) 4930. DOI: https://doi.org/10.3390/polym14224930

[13] J. Kananathan, K. Rajan, M. Samykano, K. Kadirgama, K. Moorthy, M.M. Rahman, Preliminary Tensile Investigation of FDM Printed PLA/Coconut Wood Composite, in: M.H.A. Hassan, M.H. Zohari, K. Kadirgama, N.A.N. Mohamed, A. Aziz (eds), Technological Advancement in Instrumentation and Human Engineering "ICMER 2021", Lecture Notes in Electrical Engineering, vol. 882, Springer, Singapore, 2023, 339-350. DOI: https://doi.org/10.1007/978-981-19-1577-2_26

[14] G. Carbajal-De la Torre, N.N. Zurita-Méndez, M.d.L. Ballesteros-Almanza, J. Ortiz-Ortiz, M. Estévez, M.A. Espinosa-Medina, Characterization and Evaluation of Composite Biomaterial Bioactive Glass–Polylactic Acid for Bone Tissue Engineering Applications, Polymers 14/15 (2022) 3034. DOI: https://doi.org/10.3390/polym14153034